Int Nano Lett (2014) 4:95
DOI 10.1007/s40089-014-0095-6

ORIGINAL ARTICLE

Investigations of CO_2, CH_4 and N_2 physisorption in single-walled silicon carbon nanotubes using GCMC simulation

Mohammad Ali Bagherinia · Muhammad Shadman

Received: 5 December 2013 / Accepted: 5 January 2014 / Published online: 25 February 2014

Abstract In this paper, we report N_2, CH_4 and CO_2 adsorption in single-walled silicon carbon nanotubes (SiCNTs) using grand canonical Monte-Carlo and calculate the isosteric heat of gas adsorption. The results demonstrate that at ambient temperature and high pressure, gas adsorption in these nanotubes is in the order of $CO_2 > CH_4 > N_2$ and nanotubes' order is (10,10) < (20,20) < (40,40), while this order of adsorptivity of nanotubes will be inverted for N_2 when the pressure is very low. Then, we fit our simulation results to Langmuir and Langmuir–Freundlich equations to illustrate the mechanism of gas adsorptivity. The fitting exhibits that the simulation data obtained are very close to Langmuir–Freundlich behavior, which emphasizes that the dominant adsorptivity has occurred in multi-layer adsorption. Moreover, the comparison between our simulation results and other reports, which studied these gases' adsorption on different nanoporous materials, experimentally and theoretically, is presented to illustrate that SiCNTs still have the best gas adsorptivity ability at ambient temperature and low/high pressure.

Keywords GCMC · Adsorption · SiC nanotube · Molecular simulation

M. A. Bagherinia (✉)
Department of Chemistry, Faculty of Science, Lahijan Branch, Islamic Azad University, Lahijan, Iran
e-mail: bagherinia.ma@gmail.com; mabagherinia@gmail.com

M. Shadman
Department of Chemistry, Faculty of Science, University of Zanjan, P.O. Box 45195-313, Zanjan, Iran

Introduction

The useful discovery of carbon nanotubes by Iijima [1] has opened up the possibility of synthesis of nanometer-scale, one-dimensional materials including nanowires, nanoparticles, and nanotubes [2, 3]. Silicon carbon nanotube (SiCNT) was first synthesized in 2001 [2]; furthermore, it has been improved to grow for several kinds of one-dimensional nanostructures as a tube furnace in 2002 [3] and it is the one of the most important nanotubes with many excellent properties, especially; as promising membrane for gas adsorption applications [4].

In the past decade, much of nanoscientific investigations has focused on finding new materials in nanoscale with particular properties such as high-ability natural gas adsorption capacity, owing to their supplies of energy that satisfy industrial, governmental and business agencies [5, 6].

From the environmental, an economical benefit and the predominant cause of greenhouse effect and urgent issue suppressing global warming [7, 8], a large of worldwide attentions have been reported on adsorptivity properties of carbon dioxide (CO_2), methane (CH_4) and nitrogen (N_2) (as natural gas components) on various nanoporous materials like nanotubes to reducing CO_2 global emission and remove it from natural gas and pollutant air which as mention above, they have been considered as alternative resources of energy [5, 6].

In recent years, many researchers have studied CO_2, CH_4 and N_2 adsorption, theoretically and experimentally. That in follow we are going to examplify number of them and then compare their results with our data:

Mishra et al. [9] have reported CO_2, CH_4 and N_2 adsorption properties of a zinc-based metal organic framework, which is commonly known as ZnDABCO. Yi

et al. [10] also studied these gas adsorption equilibrium isotherms on microwave-activated carbon, experimentally. Likewise, Zhang et al. [8] have presented experimental and computational studies to evaluate the adsorption-based separation of CO_2 from flue gas and natural gas using micro-porous metal organic framework Cu-TDPAT as a sorbent material. In another work, Karra et al. [11] performed atomistic grand canonical Monte-Carlo (GCMC) simulations to understand pore size, heat of adsorption, open metal sites, electrostatics, and ligand functionalization contributing to adsorption of CO_2, CO, and N_2 in MOFs: IRMOF-1, IRMOF-3, Cu-BTC, Zn_2[bdc]$_2$[dabco].

Billemont et al. [12] have studied using experiments and molecular simulations, the adsorption of CO_2 and CH_4 in nanoporous carbons in the presence of water. They observed a small volume of water; the shape of the adsorption isotherms remained similar; both the molecular simulations and experiments showed a slight decrease in the CO_2 and CH_4 adsorption amounts [12].

In 2007, Huang et al. investigated adsorption of CO_2 and CH_4 using GCMC on single-walled carbon nanotubes (SWCNTs) [5], and they proposed Harris and Yung's EPM2 [13] and the spherical models for CO_2 as different potential models.

In this paper, applying GCMC simulation, we study adsorption of CO_2, CH_4 and N_2 to calculate their adsorptivity properties in the single-walled silicon carbon nanotubes (SWSiCNTs) purly.

GCMC computational details

Following our previous work [14, 15], the GCMC simulation was adopted here for SWSiCNTs with (10,10), (20,20) and (40,40) chirality and 50 nm tube length with 17.857, 35.714 and 71.429 Å diameters, respectively, in order to consider CH_4, N_2 and CO_2 physisorption from 294 to 343 K and 1 to 21,000 kPa range of temperature and pressure, respectively. The Si–C bond length is 1.87 Å [16].

In this research, all gas molecules are treated as one-site the simplest 12-6 Lennard–Jones (LJ) potential to calculate their interactions with together and with Si and C atoms of SWSiCNT and the LJ parameters between different atoms are calculated by Lorentz–Berthelot rules. We chose classical 12-6 LJ representation according to UFF parameterization for Si and C atoms of SWSiCNTs [17], whereas for CO_2, we used the LJ potential parameters from Ref. [5], and for CH_4 and N_2 from Ref. [18], which all LJ parameters here, are listed in Table 1.

The standard GCMC simulation is a stochastic method that can compute the adsorption isotherms of various gases in each solid framework such as nanotubes, with having a constant volume (V) in equilibrium and an infinite reservoir of gases imposing its chemical potential (μ) at fixed temperature (T) [19]. In this work we used the Music code for all GCMC calculations [20]. The last half of 15 million trials was used for calculating the ensemble averages in gas adsorption simulations. The periodic boundary condition (PBC) is imposed in tube length direction. Further GCMC details are available in our previous publications [14, 15].

It should be noted in the results and discussion section, at first we present the CO_2, CH_4 and N_2 adsorption isotherms and isosteric heats which are calculated and then the gas adsorption fitting to Langmuir and Langmuir–Freundlich equations will be exhibited and in the last subsection of results, we have been compared the gas adsorptivity of gases with other published experimental and simulation data.

Table 1 The list of 12-6 LJ potential parameters of gas molecules and atoms of SWSiCNT that have used in this work

Site	σ (nm)	ε/k_B (K)	Refs.
CH_4	0.296	36.700	[18]
CO_2	0.373	147.990	[5]
N_2	0.332	30.474	[18]
Si (SiCNT)	0.383	202.429	[17]
C (SiCNT)	0.340	43.308	

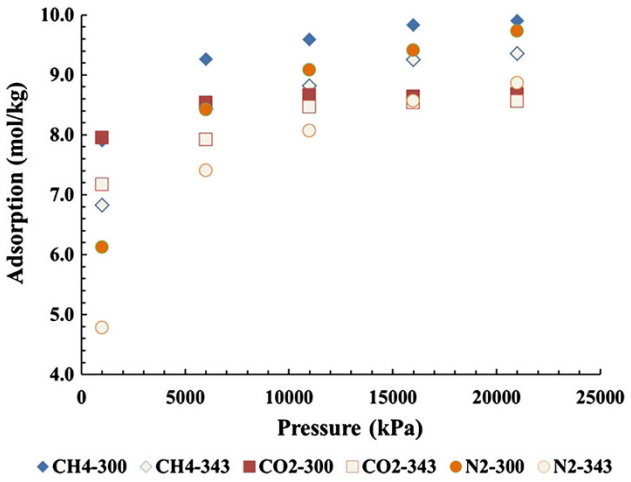

Fig. 1 CH_4, CO_2 and N_2 adsorption in (10,10) SWSiCNT at 300 and 343 K

Results and discussion

This work investigates gas adsorption properties of SWSiCNTs using GCMC.

The gases are CH_4, CO_2 and N_2. Therefore, our results are presented in some following sections.

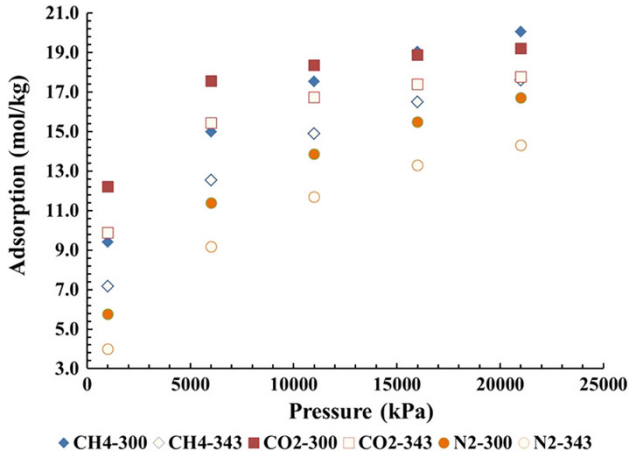

Fig. 2 CH_4, CO_2 and N_2 adsorption in (20,20) SWSiCNT at 300 and 343 K

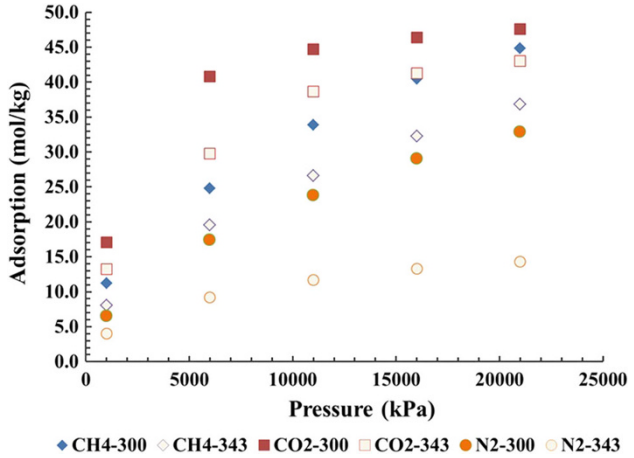

Fig. 3 CH_4, CO_2 and N_2 adsorption in (40,40) SWSiCNT at 300 and 343 K

CO_2, CH_4 and N_2 adsorptivities

At first, we show CO_2, CH_4 and N_2 adsorptivities in (10,10), (20,20) and (40,40) SWSiCNTs at 300 and 343 K at varying pressure ranges 1–21 MPa. Figures 1, 2 and 3 present the obtained data of gases in (10,10), (20,20) and (40,40) SWSiCNTs, respectively.

A result obtained from Fig. 1 shows that the gases have less adsorption, especially at higher temperature. According to Fig. 1, maximum adsorption in all gases takes place almost at 10 MPa (moderate pressure) and range of adsorptivity of gases together is low, about between 7.5 and 9.5 mol/kg. This means that (10,10) SWSiCNT has low gas adsorptivity and it seems that CH_4 and CO_2 have better adsorption, which relates to amount of adsorption as shown in Fig. 1.

From Fig. 3, we observe that the gases have more adsorptivity in (20,20) SWSiCNT than in (10,10) SWSiCNT. However, the adsorption is decreased as a function of increasing the temperature. According to Fig. 3, maximum of adsorption in all gases occurred almost at 15 MPa pressure, and range of adsorptivity of gases together was about between 13 and 19 mol/kg. This means that the (20,20) SWSiCNT has more gas adsorptivity rather than the (10,10) SWSiCNT, and CH_4 and CO_2 have better adsorptivity. Moreover, CO_2 has better amount of adsorption than CH_4 especially at low and moderate pressure (see Fig. 3).

Figure 5 also indicates that the gases have more adsorptivity in (40,40) SWSiCNT than in (10,10) and (20,20) SWSiCNTs. The gas adsorptions are decreased with increasing the temperature. Although, according to Figs. 1, 3 and 5, the maximum gas adsorptions occur in the (40,40) SWSiCNT, the range of adsorptivity of gases together in the latter nanotube is about between 10 and 45 mol/kg. This means that the (40,40) SWSiCNT has more gas adsorptivity rather than the (10,10) and (20,20) SWSiCNTs. Furthermore, it is clear that CO_2 has better adsorptivity for this reason: the most adsorptivity we can see in Fig. 5. Figure 5 shows that the (40,40) SWSiCNT can adsorb CO_2 at ambient temperature at low and moderate pressure (<10 MPa). In addition, CH_4 is adsorbed better than N_2. Consequently, the large diameter SWSiCNT can adsorb CO_2 much more than CH_4 and N_2, while small diameter SWSiCNT can adsorb CO_2 the same as CH_4. The important point is that CO_2 has more ε/k_B rather than CH_4 and N_2 (Table 1), so, its interaction with atoms of SWSiCNT nanotubes is more considerable.

Therefore, more adsorptivity of CO_2 is expected energetically. It means that natural adsorptivity directly depends on the atomic interactions.

Adsorption fitting to Langmuir and Langmuir–Freundlich equations

In the next investigation, we have fitted adsorption data to Langmuir ($\theta = \frac{\theta_m kP}{1+kP}$) and Langmuir–Freundlich ($\theta = \frac{\theta_m kP^n}{1+kP^n}$) equations, where θ is the amount adsorbed, P is the equilibrium pressure, and θ_m, k, b, n are isotherm parameters. Figures 4 and 5 present CH_4, CO_2 and N_2 plots at 300 and 343 K related to (10,10) and (40,40) SWSiCNTs, respectively. It is obvious that both figures show that the data of adsorption correspond to the Langmuir–Freundlich equation. These observations emphasize that the Langmuir–Freundlich is the best fitting that illustrates the adsorption of gases imply with varying energetic inhomogeneity in both (10,10) as smaller diameter and (40,40) as larger diameter SWSiCNTs [14, 15]. However, the gases adsorption adaptation to the Langmuir–Freundlich model can distinguish that multi-layer adsorptivity is very feasible

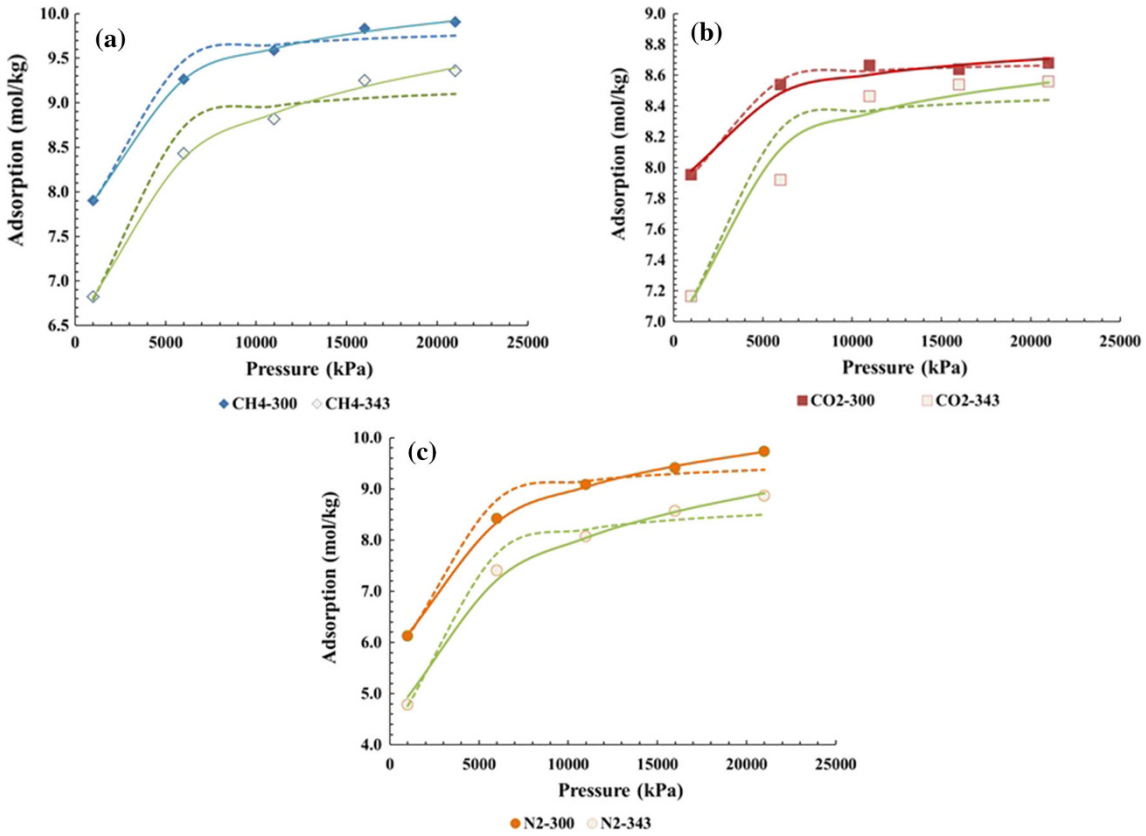

Fig. 4 The data of adsorption fitted on Langmuir (*dash lines*) and Langmuir–Freundlich (*color lines*) equations in (10,10) SWSiCNT at 300 and 343 K. **a** CH_4, **b** CO_2, **c** N_2

[14, 15]. Because the pressure is increased and temperature is lowered, additional layers are formed. This has led to the modern concept of multilayer adsorption. In Fig. 6, we can see that even in the (10,10) SWSiCNT, the secondary layer of gas adsorption is taking place. So, Langmuir's model of uni-molecular adsorption is valid here.

The comparison of gases adsorption

In this subsection, we compare the CO_2, CH_4 and N_2 adsorptions in SWSiCNTs and other nanoporous materials. Therefore, we first focus on CO_2 adsorption.

The comparison of CO_2 adsorption

Mishra et al. [9] have reported CO_2 adsorption property of ZnDABCO at 294 and 350 K, experimentally. Figure 7a that is related to 294 K, shows that ZnDABCO has more CO_2 adsorptivity than the (10,10) SWSiCNT, but it has less than the (20,20) and (40,40) SWSiCNTs. However, CO_2 adsorption properties of ZnDABCO and (20,20) SWSiCNT are very close. Figure 7b also is related to 350 K, and shows that ZnDABCO has CO_2 adsorptivity close to the (10,10) SWSiCNT, but it is less than the (20,20) and (40,40) SWSiCNTs. As a result, it seems, in relatively high temperature, SWSiCNT has good CO_2 adsorption than inorganic nanoporous materials. In fact, many inorganic nanoporous materials such as MOFs are destroyed in high temperature, while nanotubes, especially SiCNTs, have the most thermal stability [21].

Figure 7c also presents the CO_2 adsorption equilibrium isotherms reported from Refs. [8, 10] and our data at 298 K and range 1–100 kPa. This figure again indicates that the (10,10) and (20,20) SWSiCNTs have more CO_2 adsorptivity than activated carbon and Cu-TDPAT. It should be noted that our obtained simulation data values are above the simulation data values of Cu-TDPAT [8].

Karra et al. [11] reported atomistic GCMC simulations to realize the adsorption of CO_2, CO, and N_2 in IRMOF-1, IRMOF-3, Cu-BTC, $Zn_2[bdc]_2[dabco]$ at 298 K and pressure lower than 1,200 kPa. Figure 7d presents their simulation data (Ref. [11]) and our simulation results.

Another study is performed by Billemont et al. that they have been used both experimental and simulation approaches to indicate the adsorption of CO_2 on the Filtrasorb F400 activated carbon (experimental absolute adsorption) and on CS1000A and CS1000AF (simulated adsorption) as nanoporous carbons in the presence of water at 318.15 K

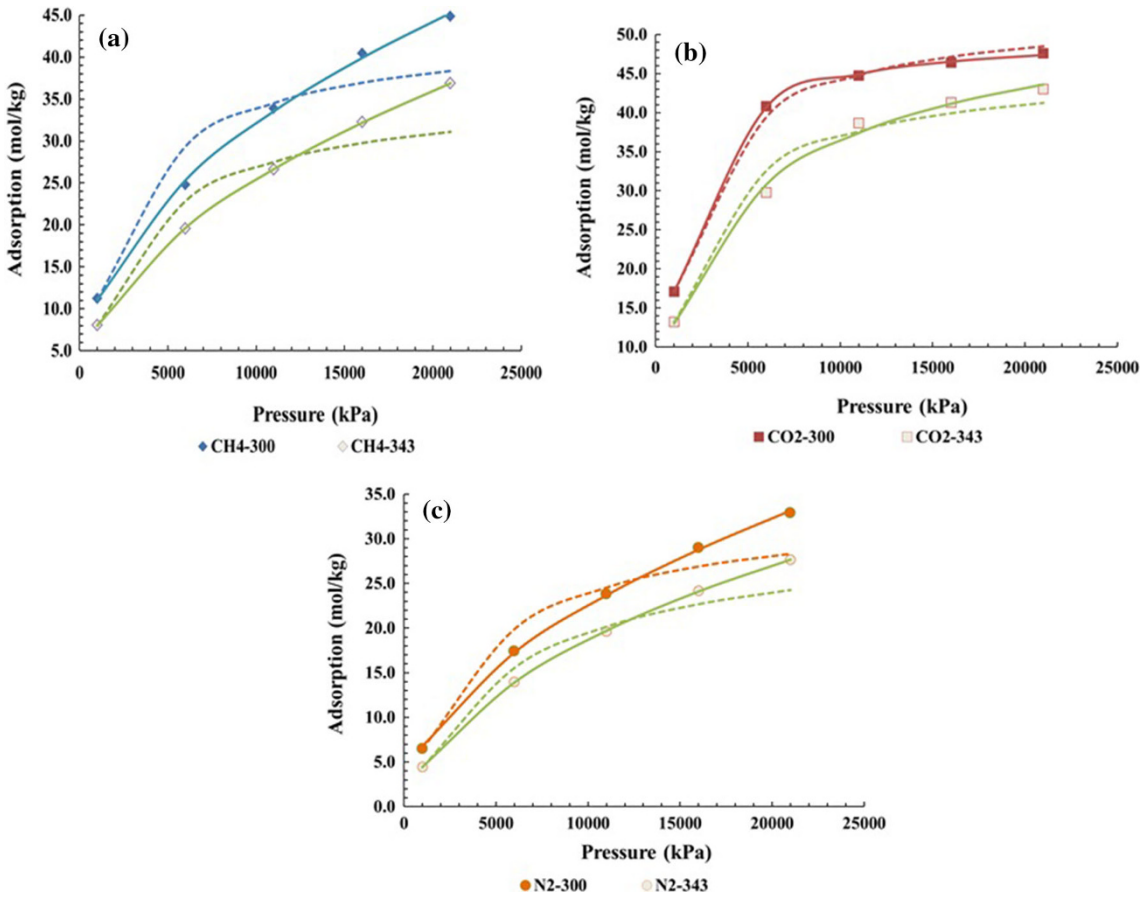

Fig. 5 The data of adsorption fitted on Langmuir (*dash lines*) and Langmuir–Freundlich (*color lines*) equations in (40,40) SWSiCNT at 300 and 343 K. **a** CH_4, **b** CO_2, **c** N_2

[12]. They show that CS1000AF has more adsorption of CO_2 than CS1000A theoretically. Then, we compare our data with simulation data of CO_2 adsorptivity on CS1000A and also Filtrasorb F400. In the section that is related to adsorption of CH_4 comparison, we will remind about Billemont et al. (Ref. [12]) research again. Figure 7e presents this comparison.

Huang et al. [5] using GCMC have investigated the adsorption of CO_2 (applying Harris and Yung's EPM2 and spherical models for CO_2 as different potential models) and CH_4 at 343 K. Their obtained data of simulation are shown in Fig. 7-e. Our results that we consider the spherical model for CO_2 at 300 and 343 K with comparing to Billemont et al. of simulation and experimental indication (Ref. [12]), illustrate that (20,20) SWSiCNT has more CO_2 adsorptivity than nanoporous carbon, but (10,10) SWSiCNT is less CO_2 adsorptivity than nanoporous carbon. In addition, the results of Huang et al. (Ref. [5]) have shown CO_2 adsorptivity close to the (10,10) SWSiCNT in the desired pressure range and at 343 K. Therefore, the (20,20) SWSiCNT can adsorb CO_2 more than nanoporous carbon and SWCNTs at the same thermodynamic conditions. As a result, Billemont et al. of simulation and experimental research (Ref. [12]) has been done at 318.15 K, and our investigation is at 300 and 343 K, and we know the adsorption decreases with increasing temperature, so, we can realize that (20,20) SWSiCNT even at 343 K has more CO_2 adsorptivity than nanoporous carbon at 318.15 K.

Consequently, as final investigation of the adsorption of CO_2, we can find that SWSiCNT with diameter large enough (diameter larger than (10,10) tube) is proper to adsorb CO_2 as compared to some MOFs, nanoporous carbon and CNTs.

The comparison of CH_4 adsorption

In our work, also, we compare CH_4 adsorptivity in SWSiCNTs with other nanoporous materials such as Cu-TDPAT and ZnDABCO as MOF, activated carbon and CNTs. At first, we report our obtained simulation data at 294 K and pressure under 3,000 kPa, with Mishra et al.

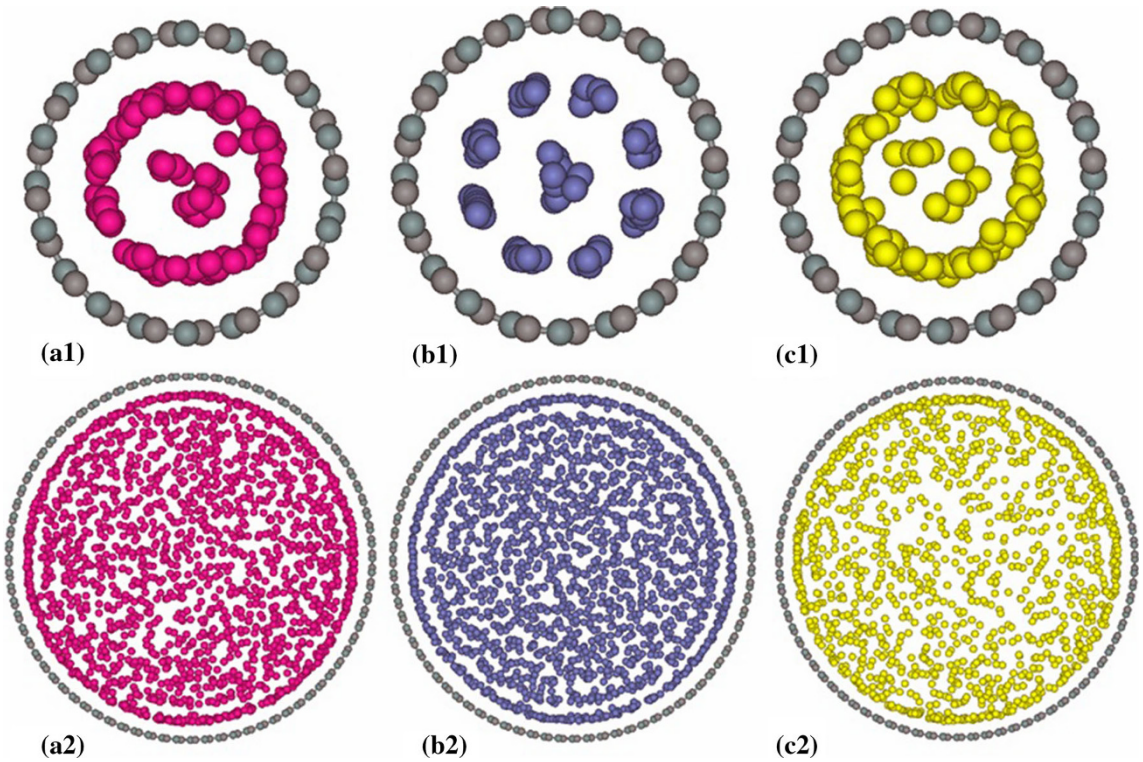

Fig. 6 The cross-section of (10,10) and (40,40) SWSiCNTs while CO_2, CH_4 and N_2 are adsorbed inside them at 300 K and 21 kPa. **a** CH_4, **b** CO_2, **c** N_2. "*1*" and "*2*" are assigned to (10,10) and (40,40) SWSiCNTs, respectively

(Ref. [9]) as experimental study that it has been considered the adsorption of CH_4 on a zinc based metal organic framework: ZnDABCO. Figure 8a illustrates the adsorption isotherms of CH_4 in this case. In Fig. 8a, we can find that CH_4 adsorptivity even in the (10,10) SWSiCNT is more than in ZnDABCO; however, our data are from simulation, and Mishra et al.'s (Ref. [9]) work is an experimental study. Furthermore, Fig. 8a, shows that CH_4 adsorptivity behavior is the same, in both ZnDABCO and SWSiCNT.

Figure 8b also compares Yi et al.'s (Ref. [10]) experimental study and Zhang et al.'s (Ref. [8]) experimental and simulation works with our simulation data at 298 K and pressure range of 0–100 kPa, while Yi et al. (Ref. [10]) represented their data on activated carbon, and Zhang et al. (Ref. [8]) reported their data on Cu-TDPAT. Figure 8b shows that considering GCMC simulation on adsorptivity of CH_4 in Cu-TDPAT and SWSiCNT, we can realize that SWSiCNT, even with (10,10) chirality is more CH_4 adsorbable than Cu-TDPAT at same thermodynamic conditions. Also, this figure emphasizes that experimental data from Ref. [10] on activated carbon are very close to experimental and simulation data from Ref. [8] on Cu-TDPAT. This is a very gratifying challenge in gas adsorption investigations, because reports contain both simulation and experimental studies on two different nanoporous materials. Simulation data and experimental data from Ref. [8] provide similar estimates of the adsorption of gases on MOFs. Also, our obtained data exhibit that SWSiCNT is a more CH_4 adsorbable nanoporous material. Therefore, we understand that this type of analysis (simulation calculations) can be accurate, while the achievement of this method can be significant, and results obtained from the simulation calculations are credible in this field.

In addition, we compare CH_4 adsorption at 300 and 343 K and pressure range 0–25,000 kPa with Ref. [12] as experimental (on Filtrasorb F400 activated carbon at 318.15 K) and simulation (on CS1000A and CS1000AF activated carbons) investigations and with Ref. [5] as simulation study (on CNTs). Figure 8c exhibits that GCMC simulation data of CH_4 on (10,10) SWSiCNT is more than GCMC simulation data of CH_4 on CNTs (Ref. [5]). In fact, CNTs have about 1 mol/kg CH_4 adsorbed value at 343 K (considering both EPM2 and spherical models of CH_4) while (10,10) SWSiCNT has about 7–9 mol/kg CH_4 adsorbed value at 343 K (considering spherical model of CH_4 in our work). However, simulation investigation on CS1000A and CS1000AF activated carbons at 318.15 K from Ref. [12] is very close to our data of

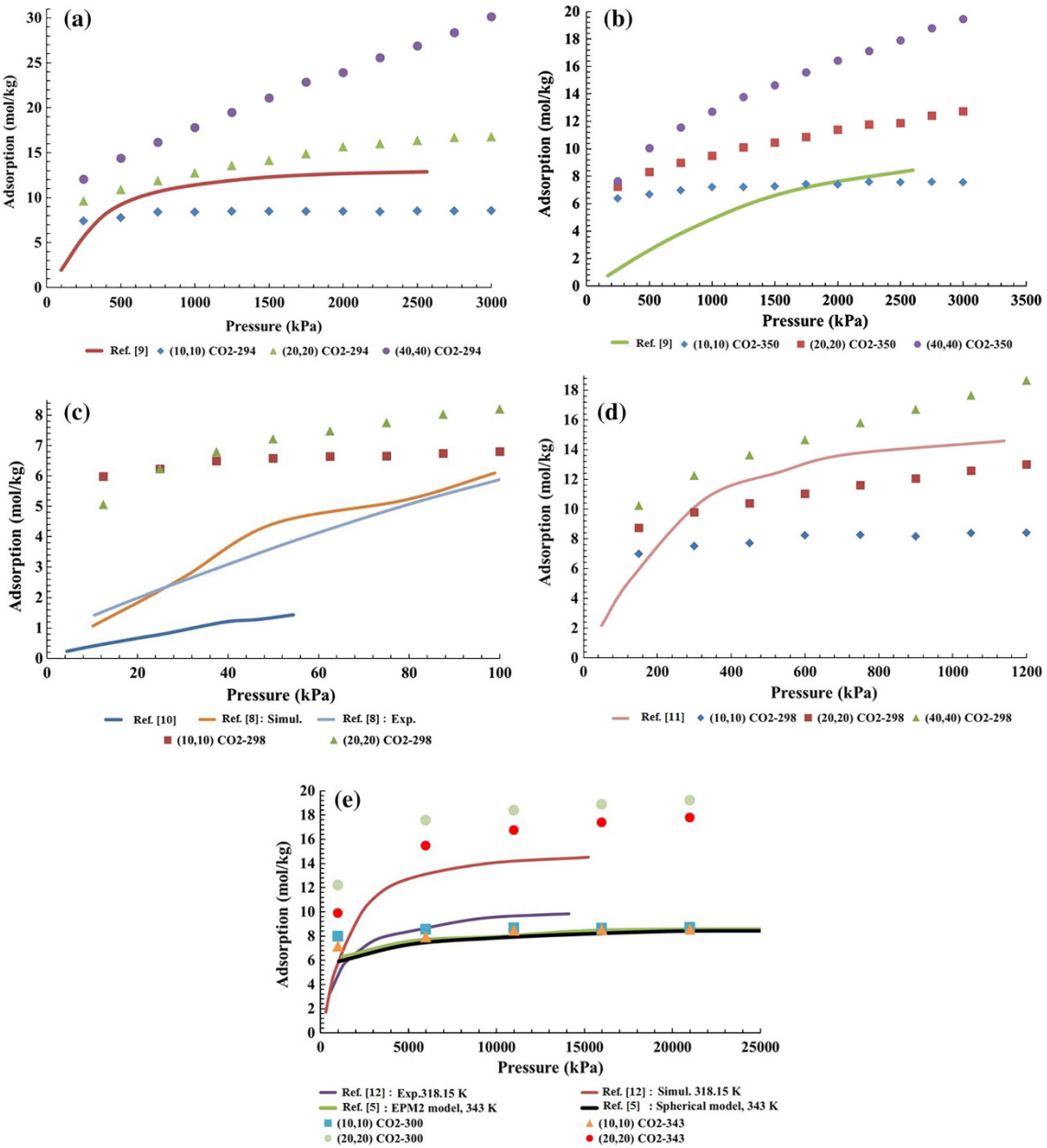

Fig. 7 **a** CO_2 adsorption property of ZnDABCO reported from Ref. [9] and our results at 294 K. **b** CO_2 adsorption property of ZnDABCO reported from Ref. [9] and our results at 350 K. **c** CO_2 adsorption equilibrium isotherm from Refs. [8, 10] and our data at 298 K and range 1–100 kPa. **d** Adsorption simulation of CO_2 from Ref. [11] that is about CO_2 adsorption in Cu-BTC and our data at 298 K. **e** Adsorption simulation of CO_2 from Ref. [12] experimental and simulation results, Ref. [5] simulation data and our data at range of 1,000–25,000 kPa

(10,10) SWSiCNT at 300 and 343 K, but (20,20) SWSiCNT, even at 343 K (that is more than 318.15 K) shows more CH_4 adsorptivity.

Finally, with considering to Fig. 8a, b and c, we can result that SWSiCNT with large enough diameter is more CH_4 adsorbable at room temperature, and also, GCMC simulation can predict suitable the CH_4 adsorption behavior, this approach can also be reliable in terms of accuracy.

The comparison of N_2 adsorption

In last comparison, we represent our N_2 adsorption from GCMC simulations with experiments reports and with few existing theoretical works.

Figure 9a exhibits our data and Mishra et al. (Ref. [9]) experimental report at 294 K under pressure of 3,000 kPa. Mishra et al. [9] present their temperature investigations

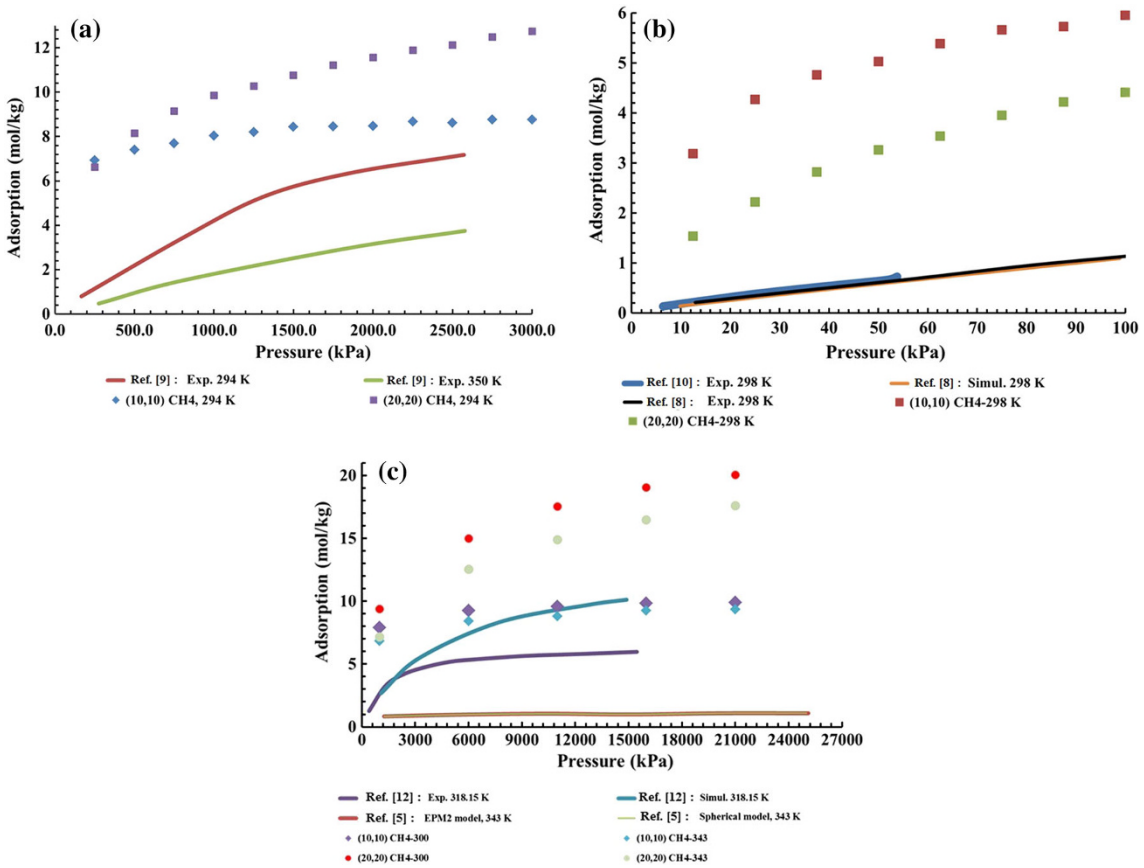

Fig. 8 **a** CH_4 adsorption property of ZnDABCO reported from Ref. [9] and our results at 294 K. **b** CH_4 adsorption equilibrium isotherm from Refs. [8, 10] and our data at 298 K and range of 1–100 kPa. **c** Adsorption simulation of CH_4 from Ref. [12] experimental and simulation results, Ref. [5] simulation data and our data at range of 1,000–25,000 kPa

and they have been resulted that ZnDABCO has a little more N_2 adsorptivity at 294 K than 350 K. Also, our GCMC simulation data of N_2 is more than Mishra et al. (Ref. [9]) reports. In Fig. 9a, we can realize that N_2 cannot more adsorbable in one type of materiel at different thermodynamics conditions. It means that with varying the thermodynamic conditions, for instance in ZnDABCO, according to Ref. [9] as experimental work, we can see that the increase of pressure cannot significantly affect nitrogen uptake, and even though with decreasing the temperature, not significant changing occur in N_2 uptake. Also, we can observe from our simulation calculations that the increase of pressure cannot have considerable effect on nitrogen uptake in (10,10) and (20,20) SWSiCNTs. Here, like CO_2 and CH_4 adsorptions compared in previous subsections, we find that N_2 adsorption behavior from simulation data is similar to experimental study.

In this paper, Fig. 9b shows interesting results. In Sect. 3.1 related to reports of gas adsorption in our work, we can see that N_2 adsorptions, at 300 K and range 1,000–21,000 kPa, are 5–30 mol/kg in (10,10), (20,20) and (40,40) SWSiCNTs (please see Figs. 1, 2, 3). But Fig. 9b exhibits our simulation of N_2 adsorption at 298 K at pressure range 0–12 kPa (very low pressure). Figures 1, 2 and 3 show that at pressure range 1,000–21,000 kPa, N_2 adsorption in SWSiCNTs is in the order of: (10,10) < (20,20) < (40,40), but at 0–12 kPa (according Fig. 9b), we can observe that N_2 adsorption in SWSiCNTs is in the order of: (10,10) > (20,20). Also, Yi et al. [10] have been studied as experimental work on activated carbon shows N_2 adsorption similar to (20,20) SWSiCNT at 298 K. This observation of N_2 adsorption can see in Fig. 9c which this latter figure also, exhibits that: (1) N_2 adsorption in SWSiCNTs are order as: (10,10) > (20,20) under 100 kPa similar to results of Fig. 8b, (2) our GCMC simulation data of N_2 adsorption in (20,20) SWSiCNT is more than Cu-TDPAT (Ref. [8]) and (3) experimental and simulation data of N_2 adsorption in Ref. [8] investigation is very close to together.

Then, from Fig. 9a, b and c we can understand that N_2 adsorption at least under 100 kPa (about 1 atm) is differ than over than 1,000 kPa (10 atm) in SWSiCNTs so that, at low pressure (about 1 atm and ambient pressure) SWSiCNT with small diameter is more N_2 adsorbable than

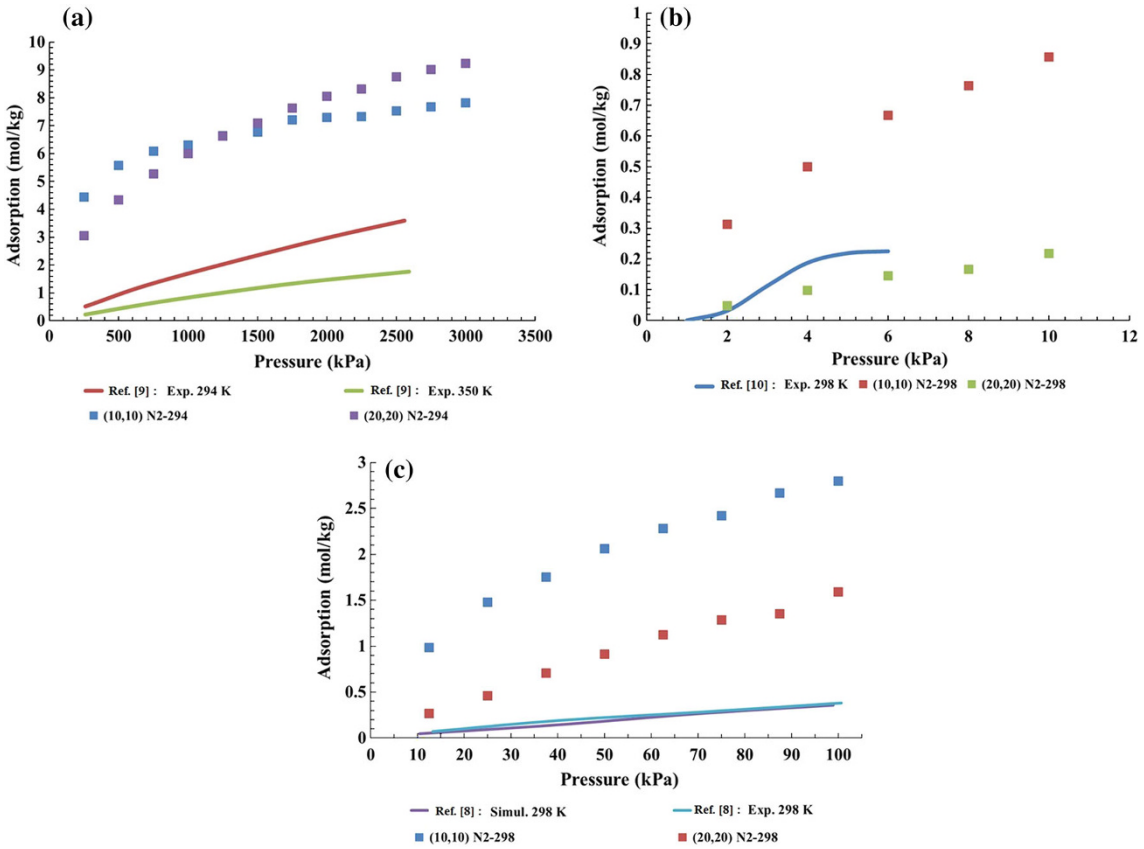

Fig. 9 **a** N_2 adsorption property of ZnDABCO reported from Ref. [9] and our results at 294 K. **b** N_2 adsorption equilibrium isotherm from Ref. [8, 10] and our data at 298 K and range of 1–100 kPa. **c** Adsorption simulation of N_2 from Ref. [12] experimental and simulation results, Ref. [5] simulation data and our data at range of 1,000–25,000 kPa

other SWSiCNT, contrariwise, SWSiCNT with large diameter is more N_2 adsorbable at pressure over 1,000 kPa (10 atm). Also, N_2 can adsorb lower than other gases because of their weakness interaction potentials with atoms of adsorbent (here SWSiCNT) and this lower adsorptivity is proved even with experimental observations.

Conclusion

This work deals with CO_2, CH_4 and N_2 physisorption in SWSiCNTs by using GCMC approach. The adsorption isotherms of gases are prepared, and interpretation of these quantities illustrates that CO_2 has more adsorption in the pure state at ambient temperate and high pressure, and with increasing the diameter of nanotube, we observe, the increase of gas adsorption, while at very low pressure this result is inverted. In addition, we compare our simulation results with other experimental and theoretical investigations, which consider these gas adsorptions on different nanoporous materials. The observations show that SWSiCNTs are the best candidates for gas adsorption.

Acknowledgments This work was supported by the Department of Chemistry, Faculty of Science, Lahijan Branch, Islamic Azad University and authors are greatly acknowledged them.

Conflict of interest The authors declare that they have no conflict of interest.

Authors' contributions MS was involved in designing the simulation work and MAB was involved in in getting the data and drafting the manuscript. MS revised the manuscript critically and MAB gave final approval for submission. Both authors read and approved the final manuscript.

References

1. Iijima, S.: Helical microtubules of graphitic carbon. Nature **354**, 56–58 (1991)
2. Pham-Huu, C., Keller, N., Ehret, G., Ledoux, M.J.: The first preparation of silicon carbide nanotubes by shape memory synthesis and their catalytic potential. J. Catal. **200**, 400–410 (2001)
3. Sun, X.H., Li, C.P., Wong, W.K., Wong, N.B., Lee, C.S., Lee, S.T., Teo, B.K.: Formation of silicon carbide nanotubes and

nanowires via reaction of silicon (from disproportionation of silicon monoxide) with carbon nanotubes. J. Am. Chem. Soc. **124**, 14464–14471 (2002)
4. Malek, K., Sahimi, M.: Molecular dynamics simulations of adsorption and diffusion of gases in silicon-carbide nanotubes. J. Chem. Phys. **132**, 014310 (2010)
5. Huang, L., Zhang, L., Shao, Q., Lu, L., Lu, X., Jiang, S., Shen, W.: Simulations of binary mixture adsorption of carbon dioxide and methane in carbon nanotubes: temperature, pressure, and pore size effects. J. Phys. Chem. C **111**, 11912–11920 (2007)
6. Basu, S., Cano-Odena, A., Vankelecom, I.F.J.: MOF-containing mixed-matrix membranes for CO_2/CH_4 and CO_2/N_2 binary gas mixture separations. Sep. Purif. Technol. **81**, 31–40 (2011)
7. Peng, X., Cao, D., Zhao, J.: Grand canonical Monte Carlo simulation of methane–carbon dioxide mixtures on ordered mesoporous carbon CMK-1. Sep. Purif. Technol. **68**, 50–60 (2009)
8. Zhang, Z., Li, Z., Li, J.: Computational study of adsorption and separation of CO_2, CH_4 and N_2 by an *rht*-type metal–organic framework. Langmuir **28**, 12122–12133 (2012)
9. Mishra, P., Mekala, S., Dreisbach, F., Mandal, B., Gumma, S.: Adsorption of CO_2, CO, CH_4 and N_2 on a zinc based metal organic framework. Sep. Purif. Technol. **94**, 124–130 (2012)
10. Yi, H., Li, F., Ning, P., Tang, X., Peng, J., Li, Y., Deng, H.: Adsorption separation of CO_2, CH_4, and N_2 on microwave activated carbon. Chem. Eng. J. **215–216**, 635–642 (2013)
11. Karra, J.R., Walton, K.S.: Molecular simulations and experimental studies of CO_2, CO, and N2 adsorption in metal-organic frameworks. J. Phys. Chem. C **114**, 15735–15740 (2010)
12. Billemont, P., Coasne, B., Weireld, G.D.: Adsorption of carbon dioxide, methane, and their mixtures in porous carbons: effect of surface chemistry, water content, and pore disorder. Langmuir **29**, 3328–3338 (2013)
13. Harris, J.G., Yung, K.H.: Carbon dioxide's liquid–vapor coexistence curve and critical properties as predicted by a simple molecular model. J. Phys. Chem. **99**, 12021–12024 (1995)
14. Shadman, M., Ahadi, Z.: Argon and neon storages in single-wall boron nitride nanotubes: a Grand Canonical Monte-Carlo Study. Fuller. Nanotub. Carbon Nanostruct. **19**, 1–13 (2011)
15. Ahadi, Z., Shadman, M., Yeganegi, S., Asgari, F.: Hydrogen adsorption capacities of multi-walled boron nitride nanotubes and nanotube arrays: a grand canonical Monte Carlo study. J. Mol. Model. **18**, 2981–2991 (2012)
16. Menon, M., Richter, E., Mavrandonakis, A., Froudakis, G., Andriotis, A.N.: Structure and stability of SiC nanotubes. Phys. Rev. B **69**, 115322–115325 (2004)
17. Li, X., Yang, W., Liu, B.: Fullerene coalescence into metallic hetero structures in boron nitride nanotubes: a molecular dynamics study. Nano Lett. **7**, 3709–3715 (2007)
18. Shadman, M., Yeganegi, S., Ziaie, F.: Ab initio interaction potential of methane and nitrogen. Chem. Phys. Lett. **467**, 237–242 (2009)
19. Binder, K., Heermann, D.W.: Monte Carlo Simulation in Statistical Physics. Springer, Berlin (2002)
20. Gupta, A., Chempath, S., Sanborn, M.J., Clark, L.A., Snurr, R.Q.: Object-oriented programming paradigms for molecular modeling. Mol. Simul. **29**, 29–46 (2003)
21. Mani-Biswas, M., Cagin, T.: Insights from theoretical calculations on structure, dynamics, phase behavior and hydrogen sorption in nanoporous metal organic frameworks. Comput. Theor. Chem. **987**, 42–56 (2012)